

Original citation:

Pešić, Ninoslav, Živanović, Stana, Dennis, Jamie and Hargreaves, James. (2015) Experimental and finite element dynamic analysis of incrementally loaded reinforced concrete structures. *Engineering Structures*, 103 .

Permanent WRAP url:

<http://wrap.warwick.ac.uk/72405>

Copyright and reuse:

The Warwick Research Archive Portal (WRAP) makes this work by researchers of the University of Warwick available open access under the following conditions. Copyright © and all moral rights to the version of the paper presented here belong to the individual author(s) and/or other copyright owners. To the extent reasonable and practicable the material made available in WRAP has been checked for eligibility before being made available.

Copies of full items can be used for personal research or study, educational, or not-for-profit purposes without prior permission or charge. Provided that the authors, title and full bibliographic details are credited, a hyperlink and/or URL is given for the original metadata page and the content is not changed in any way.

Publisher's statement:

© 2015, Elsevier. Licensed under the Creative Commons Attribution-NonCommercial-NoDerivatives 4.0 International <http://creativecommons.org/licenses/by-nc-nd/4.0/>

A note on versions:

The version presented here may differ from the published version or, version of record, if you wish to cite this item you are advised to consult the publisher's version. Please see the 'permanent WRAP url' above for details on accessing the published version and note that access may require a subscription.

For more information, please contact the WRAP Team at: publications@warwick.ac.uk

warwick**publications**wrap

highlight your research

<http://wrap.warwick.ac.uk>

Experimental and finite element dynamic analysis of incrementally loaded reinforced concrete structures

NINOSLAV PEŠIĆ^a
STANA ŽIVANOVIĆ^a
JAMIE DENNIS^b
JAMES HARGREAVES^b

^a University of Warwick, School of Engineering, Coventry CV4 7AL, United Kingdom

^b ARUP, Adv. Technology & Research Division, Blythe Gate, Blythe Valley Park, Solihull B90 8AE, United Kingdom

Submitted for publication on 11 September 2014

Accepted on 21 July 2015

ABSTRACT

This work investigates influence of damage in reinforced concrete (RC) structures on their dynamic properties through modal testing and non-linear finite element (FE) analysis. Five RC beams were designed with the fundamental flexural mode frequencies in the range of 6.5–18.0 Hz for the uncracked state. Mechanical properties of concrete, such as static and dynamic elastic moduli were determined from standard tests and ultra-sonic pulse velocity readings. The beams were incrementally loaded until the span/250 deflection limit was reached and their natural frequencies were measured from the free decay vibrations. The progressive damage reduced fundamental frequencies of tested beams by up to 25%. The non-linear FE analysis was carried out for RC beams and one two-span slab and the calculated reduced frequencies of the 1st and 2nd vibration modes were in excellent agreement with measurements. This led to the conclusion that, given that the non-linear analysis can capture degradation of dynamic stiffness due to cracking, the future dynamic performance and damage identification on the RC structure can be reliably determined from the same FE model. The results reveal potential of the combined modal testing and FE analysis to improve inspection and assessment of the in-service RC structures.

Keywords: Concrete; Modal testing; FE analysis; Structural dynamics; Damage assessment

1 Introduction

1.1 Background

The modal analysis of the in-service RC structures is gaining prominence as non-destructive damage assessment technique from the basic premise that the measured reduction of natural frequencies of vibration serves as a structural health or damage indicator. This concept brings together traditional inspection methodology, the experimental modal analysis and structural dynamic analysis for investigating structural performance and/or damage in the existing RC structures.

Among the most important parameters in the dynamic analysis and integrity assessment of any RC structure is the value of the modulus of elasticity for concrete. The distinction between the *static* and *dynamic* modulus of elasticity, both depending on the concrete mix, has already been made from small specimens and beam tests [1-3]. The static modulus, E_c , is determined from the standardised cylinder compression tests while the dynamic modulus, $E_{c,dyn}$, is obtained from the resonance tests or the ultra-sonic pulse velocity (UPV) readings [4]. Several empirical equations correlate compressive strength and static modulus of concrete to the dynamic modulus [5, 6]. The dynamic modulus of concrete is typically 10% to 40% larger than the static modulus [7].

It will be addressed in the course of our analysis whether the value of the static or dynamic elastic modulus of concrete should feature in the governing equation of flexural vibrations of RC beams. In the case of a simply supported *cracked* RC beam with the cross-sectional area and the second moment of area, $A(x)$ and $I(x)$, varying along the span, L_s , this equation has the form:

$$\frac{\partial^2}{\partial x^2} \left[E_{c/c,dyn} I(x) \frac{\partial^2 y}{\partial x^2} \right] + m_b A(x) \frac{\partial^2 y}{\partial t^2} = 0 \quad (1)$$

Here, y is the sectional displacement (deflection), x is the section coordinate along the beam span ($0 \leq x \leq L_s$), m_b is the mass per unit length of the beam and t denotes time. To calculate the frequency of the n -th mode of vibration, the closed-form solution to Eq. (1) is readily available for the simplest case when the beam cross-section is assumed to be uniform along the span:

$$f_{nc} = \frac{\pi}{2} \left(\frac{n}{L_s} \right)^2 \sqrt{\frac{E_{c/c.dyn} I_{ec}}{m_b}} \quad (n = 1, 2, 3, \dots) \quad (2)$$

In Eq. (2), the flexural stiffness of the cracked RC beams is product of the elastic modulus of concrete and the effective second moment of area defined by the Eurocode 2 [8, 9] as:

$$I_{ec} = \alpha I_{c1} + (1 - \alpha) I_{c2} \quad (3)$$

where I_{c1} and I_{c2} are the second moment of areas of the gross and cracked RC section, respectively, while $0.60 \leq \alpha \leq 0.80$ is the load parameter [9]. This approximation of the second moment of area might be suitable for estimating the frequency reduction on RC beams at the design stage but is not applicable for damage identification on the more complex structural elements or when the cumulative effects of incremental loading need to be assessed.

In an improvement over Eq. (3), a continuous function for reduced flexural stiffness was proposed for damage identification on cracked RC beams with known frequencies [10]. Three damage parameters, denoted as α , β and n represent reduced stiffness of the cross-section, the length and the shape of the beam damaged zone and are iteratively determined by equating the measured frequencies with those calculated from the 2D segmental model of the beam. These analysis steps outline the basics of the model updating technique that needs to be expanded for dynamic analysis of geometrically more complex RC structures warranting finite element (FE) modelling and analysis.

It was observed from the experimental modal analysis of the incrementally damaged RC beams and slabs [8, 11-13] that their frequency of the 1st vibration mode can be reduced up to 30%

when the yielding of the tensile reinforcement occurs [14, 15]. Such magnitude of frequency reduction, being a consequence of structural damage, gave rise to the concept of damage identification by means of modal testing [16, 17]. The method is applicable to RC structures for a range of problems from vibration serviceability of the concrete floor slabs in buildings to the assessment of bridges.

The FE model updating technique has already been used for accurate evaluation of the dynamic properties of the field-tested concrete structures that exhibit linear dynamic behaviour [18]. This work will further examine the benefits of simultaneous use of the experimental modal analysis and non-linear FE analysis for the structural assessment of traditional RC beams, slabs or other types of structures whose natural frequencies inevitably reduce due to the load-induced cracks in concrete. As cracking introduces non-linear response of RC structures, their structural performance and dynamic behaviour cannot be accurately assessed nor predicted by means of linear analysis [19, 20].

1.2 Research significance and objectives

The case now exists to expand the FE model updating methodology to the non-linear analysis of cracked RC beams and more complex structural elements modelled with solid 2D/3D or shell elements. Once sufficiently accurate natural frequencies are computed from the updated FE models, zones with structural damage could be identified from the same models using parameters that define the non-linear constitutive law for concrete.

The concept will be studied through the modal testing of five RC beams with different span/depth ratios and through the non-linear FE analysis of their 2D/3D models. The investigated points are:

- time-development of the concrete strength and static and dynamic modulus of elasticity;
- the rate of frequency reduction in RC beams with the increase in the applied loading;

- influence of the number of load cycles on the frequency reduction in RC beams;
- the accuracy of the FE analysis in predicting natural frequencies of cracked RC beams and identification of the load-induced damage in concrete.

For further correlation of results from the experimental modal testing and dynamic analysis with the extent of damage in RC structures, the non-linear analysis will also be performed on the FE models of an independently tested two-span RC slab [12].

2 Experimental programme

Five RC beams were incrementally loaded and their modal properties determined after each load-unload step. This section reports on the mechanical properties of concrete, the experimental configuration of RC beams and, finally, the results from their modal testing.

2.1 Properties of concrete

Details of the concrete mix and the curing regime are provided in Table 1. Compressive strength of concrete was evaluated as the average from three 100 mm cubes crushed in the period from 7 to 250 days after casting. Cylinder compressive strength was obtained at the age of concrete of 32 and 105 days and the static elastic modulus at the age of 32 days (this is comparable to the 28-days reference age of concrete in codes of practice). Cement CEM-II/B-V contained 30% fly-ash which, due to its slower hydration rate, added to the modest compressive strength gain after the age of 20 days. Time development of the concrete compressive strength until the age of 250 days is shown in Fig. 1. The 32-day characteristic cube and cylinder compressive strengths ($f_{ck,cube} \approx 48$ MPa and $f_{ck} \approx 43$ MPa) place this concrete between the “C35/45” and “C40/50” Eurocode 2 classes [9].

Using the averaged UPV readings, v_p , on 300, 400 and 500 mm long prisms with the same cross-sections as the tested beams (Section 2.2), the dynamic modulus of concrete was evaluated from the following relation:

$$E_{c,dyn} = \rho_c v_p^2 \frac{(1 - 2\nu)(1 + \nu)}{1 - \nu} \quad (4)$$

in which the Poisson's coefficient was adopted as a constant $\nu=0.20$ while the density of concrete cubes varied with time (due to drying) within the range of $2300 \geq \rho_c \geq 2250 \text{ kg/m}^3$.

Table 1. Details of the concrete mix.

Material into 1 m^3 of concrete volume	Mass [kg]	Volume [m^3]
Cement CEM II/B-V + SR	380	0.140
Aggregate		
0-4 mm (quartz)	895	0.338
4-20 mm (quartzite)	895	0.350
Water (W/C = 0.44)	168	0.168
Plasticiser CSP340	2.0	0.002
Air content (estimated)	/	0.002

Indoor curing, humidity = 55%:
wet hessian applied for 14 days only.

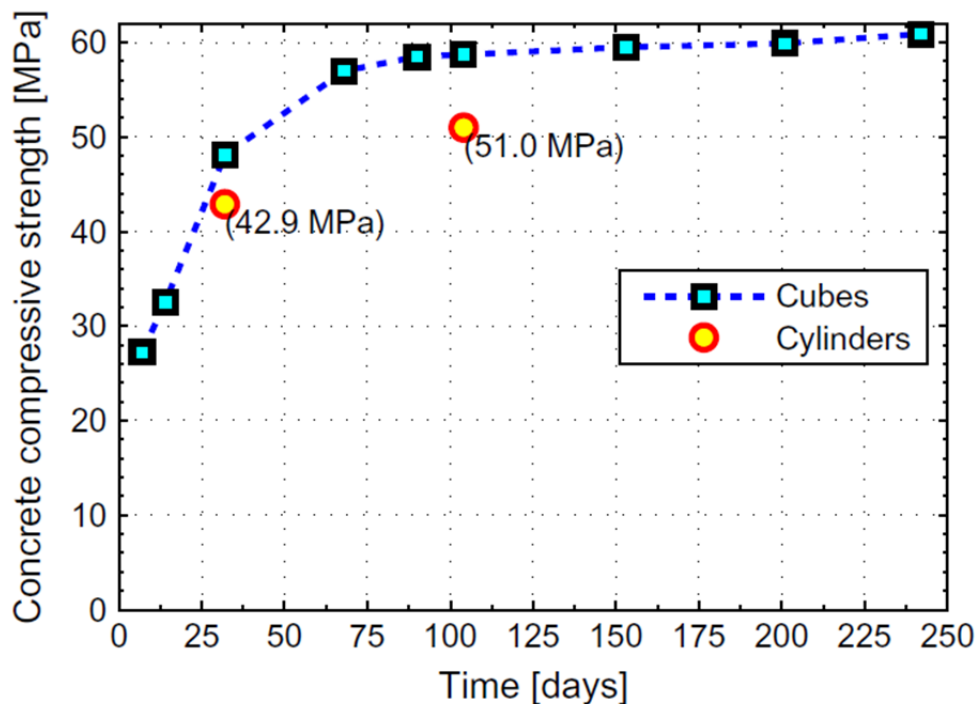


Figure 1: Development of the concrete compressive strength with time.

The static modulus of elasticity was experimentally determined as $E_c \approx 30.5 \text{ GPa}$. The Eurocode 2 equation $E_c = 22.0 (f_{cm}/10)^{0.30} \text{ [GPa]}$, in which $f_{cm} = f_{ck} + 8 \text{ [MPa]}$ is the mean characteristic compressive strength of concrete, over-estimates the experimental E_c value by nearly 20%. A

much better estimate of the static modulus was made using the empirical formula of Noguchi et al. [21]:

$$E_c = 33.5 k_1 k_2 (\rho_c/2400)^2 (f_{cm}/60)^{1/3} \quad [\text{GPa}] \quad (5)$$

Eq. (5) takes into account not only the compressive strength of concrete but also its density at the age of 28 days, $\rho_c \approx 2286 \text{ kg/m}^3$, and the type of aggregate and cement through the correction coefficients $k_1=0.95$ (quartzite aggregate) and $k_2=1.10$ (high volume fly-ash cement) giving finally the value of $E_c \approx 30.0 \text{ GPa}$.

The values of the 32-day static modulus from the cylinder tests, E_c , and the time-development of the dynamic modulus of concrete from the UPV readings, $E_{c,dyn}$, are plotted in Fig. 2. After 60 days of age, the measured UPV in dry concrete was nearly constant at $v_p \approx 4.40 \text{ km/s}$ and Eq. (4) then gives the dynamic modulus value of $E_{c,dyn} \approx 40.1 \text{ GPa}$. Small reduction in the dynamic modulus of concrete at the age of concrete between 60 and 90 days is attributed to the reduction of concrete density due to drying. For the age of concrete beyond 90 days, the dynamic to the 32-day static modulus of elasticity ratio becomes nearly constant:

$$r_e = E_{c,dyn}/E_c \approx 1.32 \quad (6)$$

2.2 RC beams setup

The geometric data of the five simply supported RC beams are provided in Table 2. The chosen span-to-depth ratios between 27.5 and 45.0 gave the fundamental natural frequencies that are near and beyond the typical values for the long-span RC floor slabs and beams in building construction. Adopting the experimental value of the static elastic modulus, $E_c=30.5 \text{ GPa}$, the predicted 1st mode frequencies of RC beams in their non-cracked state were in the range from 6.5 to 18.0 Hz. Values in Table 2 are from the FE analysis ($f_{1,FE}$) and segmental analysis method that was, in the considered cases, also applicable to simply supported beams with and without overhangs (Appendix A, $f_{1,a}$). With the yielding and the ultimate tensile strengths of reinforcing

bars measured as 555 MPa and 615 MPa, respectively, the cross-sectional yielding bending moment capacity is $M_y \approx 3.00$ kNm and the yielding load level for each beam is simply estimated as $P_y = 4M_y/L_s$.

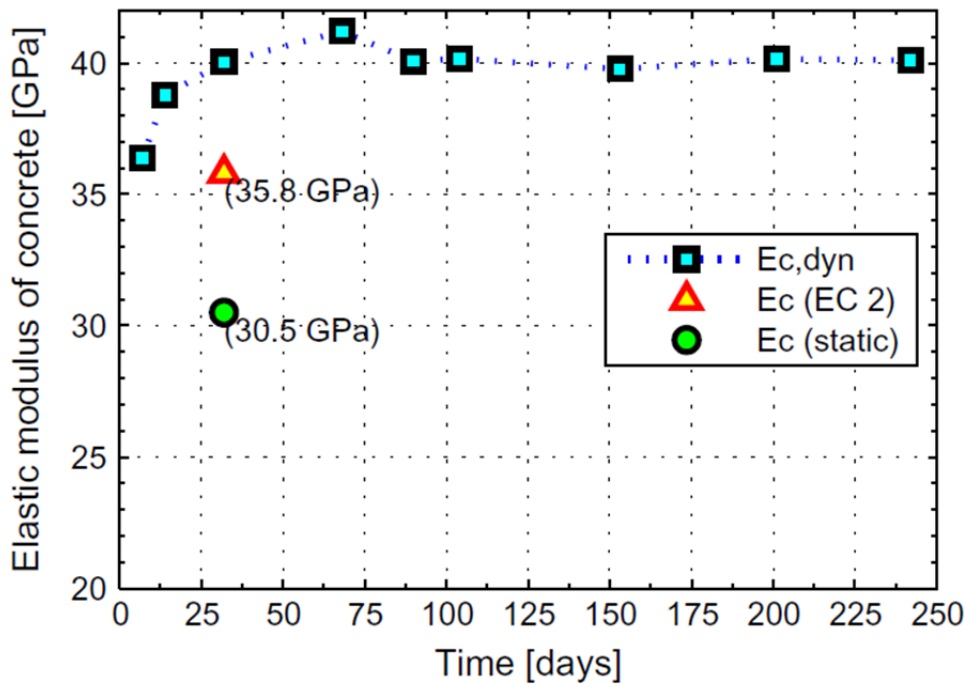


Figure 2: Static and dynamic modulus of concrete (time development).

Table 2. Geometry of the tested RC beams.

Beam no.	Length L [m]	Span L_s [m]	L_s/h	Frequency	
				$f_{1,FE}$ [Hz]	$f_{1,a}$ [Hz]
1	4.00	3.80	31.7	14.0	13.7
2	4.70	4.50	37.5	10.0	9.8
3	5.60	5.40	45.0	6.6	6.8
4	4.70	3.30	27.5	18.0	17.1
5	5.60	3.80	31.7	12.5	13.1

Cross-section dimensions:

width

$b = 300$ mm

height

$h = 120$ mm

concrete cover

$c = 25$ mm

Area of three $\varnothing 10$ mm rebars:

$A_s = 235.6$ mm²

RC beams were subjected to the symmetric three point load bending tests with one support fixed and the other made as the low-friction bearing. The incremental loading was applied using a single 10 kN capacity hydraulic jack and the static deflections were measured with the micro-meter at the peak of each loading cycle and after unloading. To cover the deformation

range of practical interest, the beams were loaded until the mid-span deflection reached the $L_s/250$ limit.

Low-amplitude vibrations were induced by the instrumented 5.5 kg Dytran 5803A sledge hammer with 5 impacts at the quarter span points. The vibration responses were recorded after each impact with Dytran 3166B1 piezometric accelerometers having nominal sensitivity of 500 mV/g and the measurement grid is shown in Fig. 3. The experimental setup was the same for all beams including the frame supports with the purpose made bearings, accelerometers and the load cell as shown in Fig. 4. For data acquisition, NI LabView software and hardware consisting of two 9234 cards and cDAQ-9172 chassis were used. During each step, the loading was kept constant for ~ 30 min (to stabilise flexural cracks) before the frequencies were measured on the unloaded beam. Due to the short duration of loading, concrete shrinkage and creep had negligible effects on the dynamic properties of beams. To assess the influence of the repeated load cycles on the frequency reduction, RC Beam 5 was also subjected to the loading scheme involving 1, 10 and 100 constant load-unload cycles at 50% of the yield load level of 1.60 kN.

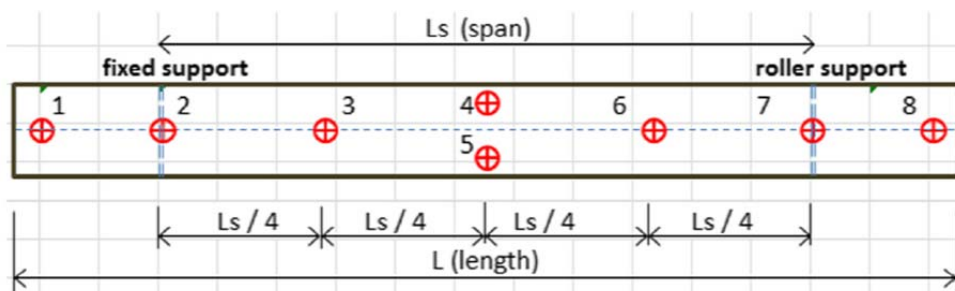


Figure 3: Positions of 8 accelerometers, \oplus , on each tested RC beam.



Figure 4: Experimental setup: (a) RC Beam 4 with accelerometers; (b) RC Beam 5 with the load cell installed at the mid-span; (c), (d) and (e) installed accelerometers and typical pattern of flexural cracks near the mid-span point.

2.3 Modal analysis results

After each load-unload cycle, free vibration responses of RC beams were recorded at the sampling rate of $f_s=1652$ Hz. For every beam, the natural frequencies were obtained from the averaged Fourier spectra of five acceleration time histories recorded for 8 s after hammer impact. All beams were subjected to the incremental loads P_i and Table 3 shows the gradual reduction in measured frequencies of the 1st and 2nd vibration modes, $f_{1,i}$ and $f_{2,i}$, respectively, with the index i denoting the load step. The predicted frequencies of the 1st mode of vibration for the non-loaded RC beams (see Table 2) are in excellent agreement with the frequencies measured before any loading was applied, $f_{1,i=0}$. For the load levels below yielding point, P_y , the gradual shifts in the natural frequencies of the 1st and 2nd modes, as identified on all tested beams, are plotted in Fig. 5.

Table 3. Measured 1st and 2nd natural frequencies, $f_{1,i}$ and $f_{2,i}$ of RC beams subjected to different load levels, P_i ($i=0,1,2,3\dots$).

RC beam	Load-unload cycle no.															
	$i=$		0	1	2	3	4	5	6	7	8	9	10	11	12	13
No.1	P_i	[kN]	0.00	1.25	1.61	1.85	2.11	2.40	2.60	2.87	3.01	3.26	3.54	3.72	4.07	4.96
	$f_{1,i}$	[Hz]	14.0	13.5	13.2	12.9	12.7	12.4	12.1	11.9	11.6	11.5	11.4	11.2	11.1	10.3
	$f_{2,i}$	[Hz]	52.6	52.0	51.7	51.4	51.1	50.6	49.9	49.6	48.8	48.4	48.0	47.4	46.9	45.0
No.2	P_i	[kN]	0.00	1.31	1.43	1.67	1.98	2.20	2.46	2.55	3.30	-	-	-	-	-
	$f_{1,i}$	[Hz]	10.1	8.72	8.60	8.50	8.43	8.27	8.06	7.82	7.73	-	-	-	-	-
	$f_{2,i}$	[Hz]	40.0	37.6	37.5	37.2	36.5	36.1	35.5	34.7	34.2	-	-	-	-	-
No.3	P_i	[kN]	0.00	0.34	0.45	0.55	0.67	0.82	0.95	1.09	1.26	1.41	1.64	2.20	-	-
	$f_{1,i}$	[Hz]	5.95	5.82	5.79	5.74	5.71	5.68	5.64	5.54	5.46	5.40	5.30	5.05	-	-
	$f_{2,i}$	[Hz]	23.9	23.6	23.5	23.4	23.3	23.2	23.1	22.9	22.6	22.4	22.2	20.9	-	-
No.4	P_i	[kN]	0.00	0.50	1.20	1.50	1.95	2.45	3.00	3.45	4.00	4.60	4.90	5.50	6.00	7.00
	$f_{1,i}$	[Hz]	16.9	16.8	16.6	16.5	16.1	15.9	15.6	15.1	14.2	13.8	13.3	13.3	13.2	13.2
	$f_{2,i}$	[Hz]	56.8	56.7	56.6	56.5	56.3	56.3	56.2	55.6	55.4	53.9	53.1	53.1	52.8	52.5
No.5	P_i	[kN]	0.00	1.50	1.60	1.60 ^a	1.60 ^b	3.00	4.50							
	$f_{1,i}$	[Hz]	12.6	12.3	12.2	12.1	11.9	11.3	10.4							
	$f_{2,i}$	[Hz]	36.5	36.0	35.9	35.9	35.8	34.9	34.1							

^a 10 load-unload cycles.

^b 100 load-unload cycles.

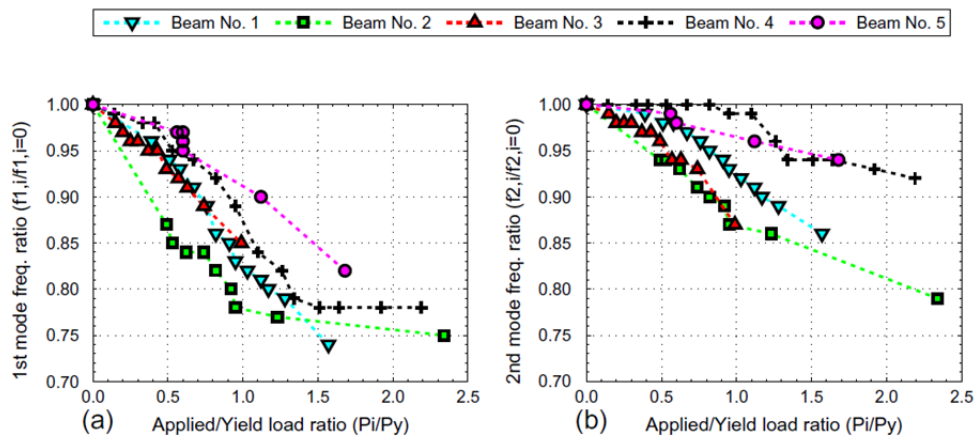


Figure 5: 1st and 2nd mode frequency reduction rate vs. the applied/yielding load ratios P_i/P_y .

Similarly to the previously reported findings [11, 15], the frequency reduction is proportionally larger for the starting load increments. Only near and after the yielding level is reached, the rate of reduction is slowed down. This is verified from the graphs showing the 1st and 2nd mode frequency ratios, $f_{1,i}/f_{1,i=0}$ and $f_{2,i}/f_{2,i=0}$, against the applied to yielding loading ratio, P_i/P_y (Fig. 5). The frequency reduction trend for RC beam 5 exhibits a discrete drop at the 1.60 kN load at which 100 load-unload cycles were applied. This cyclic loading was at relatively low level (approx. 55% of the yield load) at which no significant cumulative damage was observed. After the beam was subjected to two additional cycles at 3.0 kN and 4.5 kN, the frequency reduction resumed in the same manner as observed on other beams.

With the deflected shape of the loaded beams resembling the shape of the 1st vibration mode, the relative magnitude of the frequency reduction near the yielding point ($P_i/P_y \approx 1.0$) is larger for the 1st mode (between 10% and 25% of $f_{1,i=0}$) than for the 2nd mode (between 2% and 15% of $f_{2,i=0}$). From the practical point of view, the natural frequencies of the first two vibration modes need to be clearly identified if the shifts in the measured frequencies caused by damage in concrete are to be utilised in structural health assessment. To demonstrate this approach, frequency shifts from the initially unloaded to the yield load level are plotted in Fig. 6.

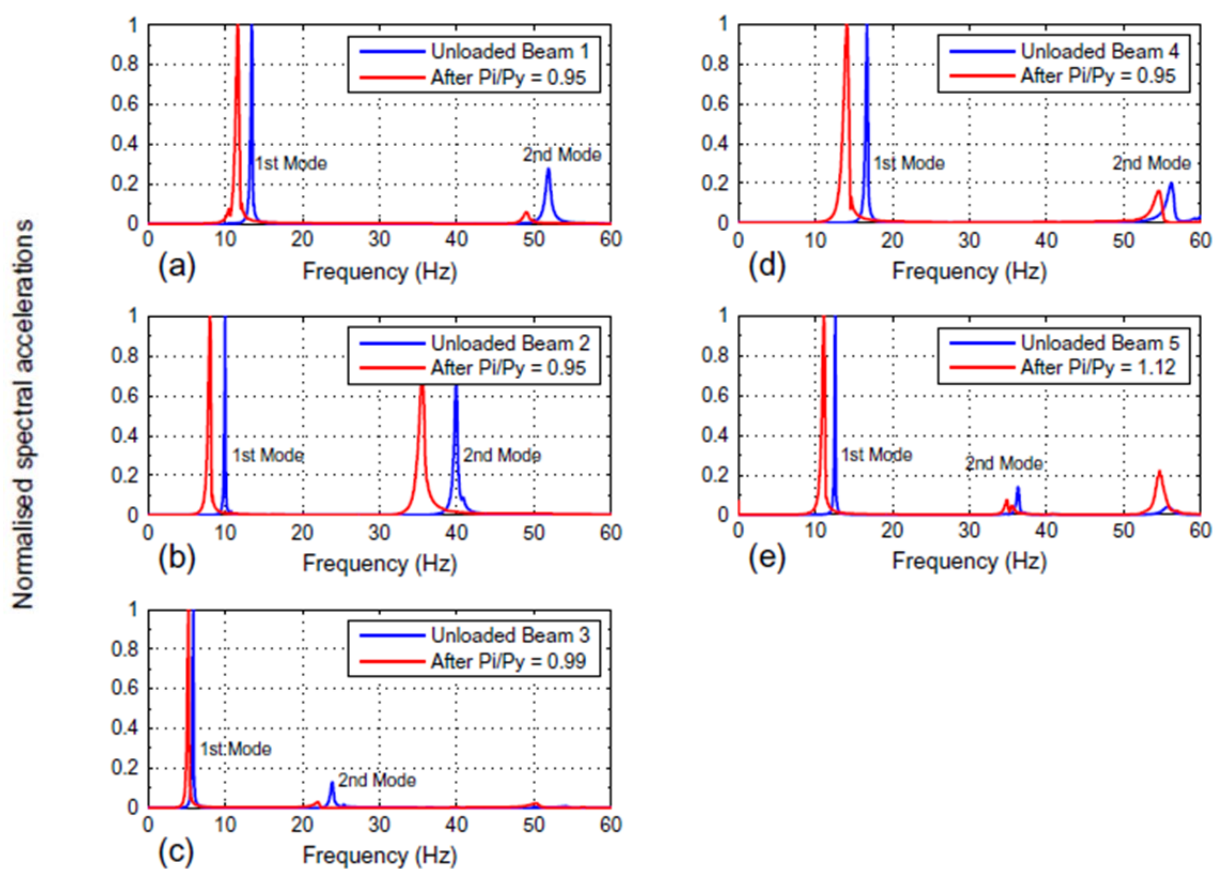


Figure 6: Frequency shifts from the FFT spectra of the vertical accelerations recorded at the quarter-span points for RC Beams 1 to 5 before and after damage (a)–(e).

3 Analysis and FE modelling

3.1 FE analysis of the RC beams

Finite element analysis of the tested RC beams was performed using the FE analysis software ABAQUS [22]. The non-linear concrete behaviour in tension and compression was modelled by the tension stiffening and damage plasticity models [23]. Two constitutive models for concrete

in tension available, the smeared cracking (SCM) and the damage plasticity model (DPM), account for the reduction of stiffness in concrete by reducing the effective modulus of elasticity when the total tensile strain exceeds the value corresponding to the peak tensile strength. The main difference is that DPM features the tensile damage variable that can take values $0 \leq d_t \leq 1.0$. This scalar, introduced in the post-peak tension stress–strain law, allows for further analytical reduction of the elastic modulus when concrete is subjected to the repeated or incremental loading. Assuming the linear post-peak stress–strain relationship for concrete in tension, $\sigma_c - \epsilon_{ct}$, and the total tensile strain expressed as the sum of the elastic and inelastic (non-recoverable) strain, $\epsilon_{ct} = \epsilon_{ct,e} + \epsilon_{ct,p}$, the mathematical reduction of the elastic modulus as a function of the isotropic tensile damage variable, $E_{c,i} = E_c(1 - d_t)$, is illustrated in Fig. 7. In the FE analysis, the change of $E_{c,i}$ is the most influential factor for the calculation of the reduced natural frequencies of any RC element or structure.

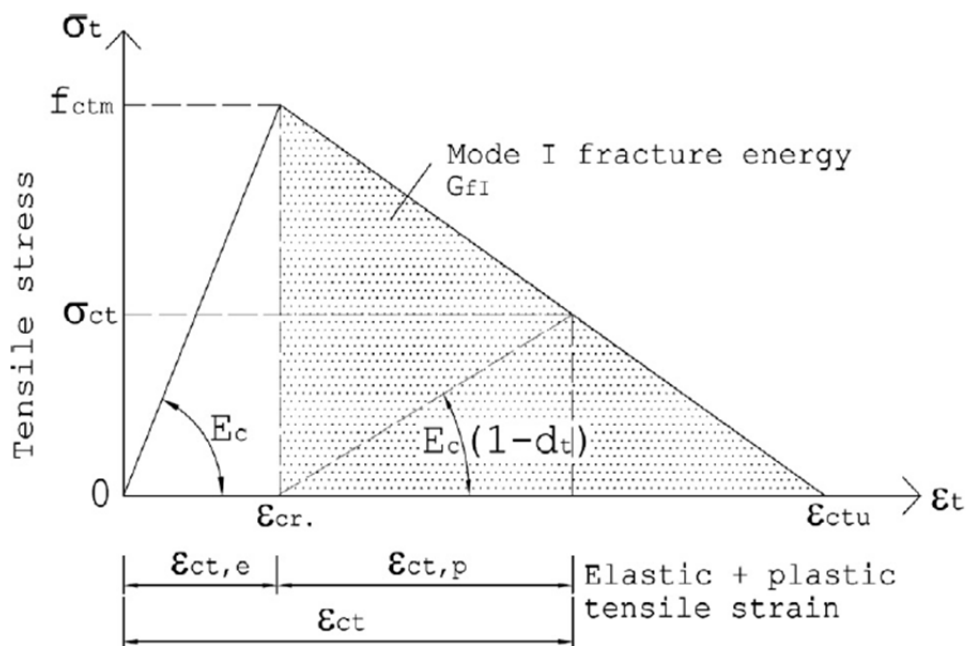


Figure 7: Adopted constitutive model for concrete in tension.

The characteristic compressive strength of concrete adopted in the analysis of RC beams was $f_{ck} = 53$ MPa; this value is representative of the cube strengths achieved during the testing period between 60 and 90 days after casting. The dynamic analysis was insensitive to the

adopted value of f_{ck} because the maximum compressive stresses in concrete from the applied loading were considerably lower (from the cross-sectional analysis, ~ 15 MPa at yielding). The stress–strain law for concrete in compression was defined by the Eurocode 2 [9] equation:

$$\sigma_c = f_{cm} \frac{k\eta - \eta^2}{1 + (k - 2)\eta} \quad (7)$$

where $k = 1.05E_{cm}|\varepsilon_{c1}|/f_{cm}$;
 $\eta = \varepsilon_c/\varepsilon_{c1}$;
 ε_{c1} is the strain at the peak compressive stress;
 σ_c is compressive stress at the given strain ε_c .

Two- and three-dimensional FE models of the tested RC beams were analysed with a number of varying parameters listed in Table 4. Variables include the choice of 2D (4- and 8-noded plane stress), or 3D (8-noded hexagon) elements, reinforcement modelling (embedded truss elements or Abaqus-rebars) and the elastic modulus, tensile strength and fracture properties of concrete.

Table 4. FE analysis methodology and variables in the parametric study.

Finite element models:	2D solid 3D solid	4- or 8-noded plane stress elements. 8-noded C3D8 hexahedral elements.			
Reinforcement modelling:	R4/E8 R4/R8	T3D2 elements embedded in 4/ 8-noded 2D/3D solids. Rebars embedded in 4/8-noded 2D/3D solids.			
Concrete constitutive laws:	SCM DPM	Smearred cracking with "tension stiffening". Damage plasticity model.			
Parametric range for FE model updating		lower	upper		
Concrete mechanical properties:		bound	bound	(best fit)	Units
modulus of elasticity	E_c	27.0	34.5	29.0	[GPa]
tensile strength	f_{ctm}	2.20	3.35	2.50	[MPa]
ultimate tensile strain	ε_{cu}	1000	2400	1400	10^{-6}
max. crack opening displacement	w_r^{ck}	0.04	0.14	0.07	[mm]
mode I fracture energy	G_f	0.09	0.16	0.11	[N/mm]

The initial estimate for the tensile strength of concrete was based on the Eurocode 2 formula (Table 3.1 in [9]) that uses the characteristic 28-day compressive strength:

$$f_{ctm} = 0.30f_{ck}^{(2/3)} \approx 3.35 \text{ MPa} \quad (8)$$

It was subsequently found that better correlations with the measured frequencies are obtained when the concrete tensile strength in the FE model is lower than the value given by Eq. (8). The

effects of several other variables and analysis factors were also examined in the parametric study. For concrete, these included the starting value of the elastic modulus, E_c , and parameters that define its post-cracking behaviour like the Mode I fracture energy, G_{fi} , the maximum crack opening, u_t^{ck} , and the ultimate (failure) tensile strain, ϵ_{ctu} . The choice between 2D or 3D solid models and the method of modelling internal reinforcement did not have significant influence on the computed frequencies of RC beams. Example in Fig. 8 is from 3D analysis of RC Beam 2 after the 2.55 kN load-unload step.

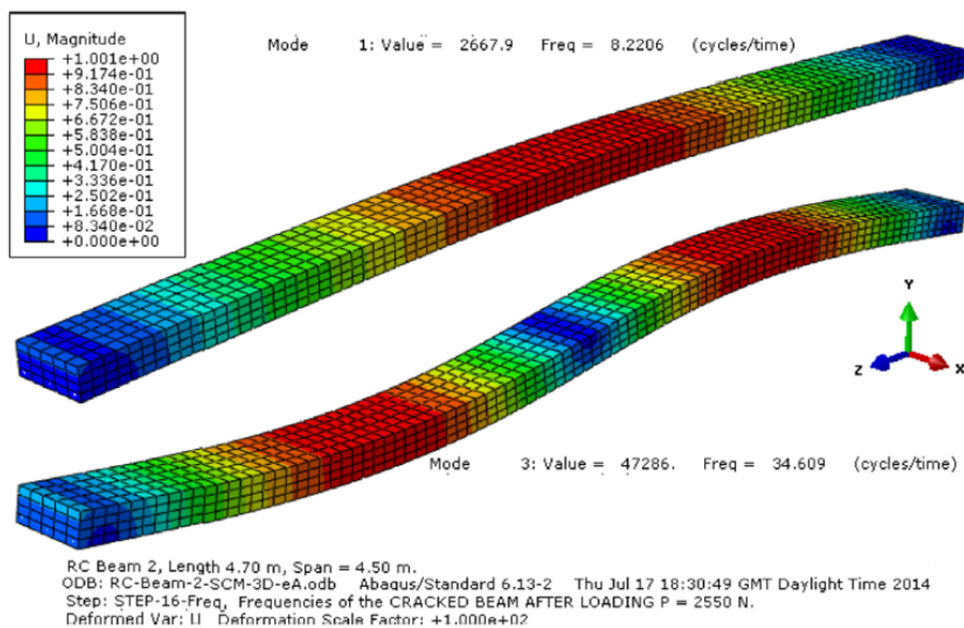


Figure 8: 1st and 2nd vibration modes of RC Beam 2 after 2.55 kN load-unload step ($i=7$, Table 3).

Variations in the 2D/3D mesh densities, with element sizes from 20 to 50 mm also did not have substantial qualitative or quantitative impact on the prediction of frequencies. The presented results are from the FE models featuring uniform mesh with the element lengths and heights of $l_m=50$ mm and $h_m=30$ mm, respectively. On the other hand, the FE models were most sensitive to the changes in the modulus of elasticity and tensile strength of concrete. The ranges of parameters used in the model updating are provided in Table 4 together with the identified values that best matched the experimentally measured frequencies of the first two vibration modes.

The accuracy of 5% to 10% against the measured frequencies of the 1st and 2nd vibration modes was achieved in the FE parametric study with the values of the elastic modulus of concrete adopted as $E_c \approx 29.0\text{--}29.5$ GPa (nearly equal to the experimental static modulus value) and the tensile strength in the region $2.30 \leq f_{ct} \leq 2.50$ MPa (at the lower bound values defined in the Eurocode 2 [9] as $f_{ct,0.05} = 0.70 f_{ctm} \approx 2.35$ MPa). For the 1st vibration mode, the load-dependent frequency reductions computed with the selected “best fit” parameter values of the mechanical properties of concrete are plotted for all beams in Fig. 9. If the elastic modulus and tensile strength are outside of these ranges, the calculated frequencies deviate considerably from the measured values. For example, Fig. 10 illustrates the load-induced frequency reduction from FE modal analysis of Beam 1 with the varying concrete tensile strength:

$$f_{ctm} \geq f_{ct} \geq 0.50 f_{ctm}.$$

Almost as a rule, in the force-controlled non-linear FE analysis, all models of tested RC beams initially exhibit somewhat higher than experimentally observed dynamic stiffness. In the case of Beam 3, the experimental frequency reduction line suggests that a minor flexural damage was already present before the load testing. However, once the applied loading caused further damage, the numerically predicted frequency reduction rate was, in absolute terms, in excellent agreement with the experimentally measured values. Fig. 9 also reveals that, for predicting vibration frequencies of damaged RC beams, the smeared cracking model outperforms less reliable damage plasticity model. While DPM provided quite accurate estimate of the beam deflections (the example load–deflection plot in Fig. 11 is for RC Beam 3), it keeps a much higher stiffness of concrete immediately after unloading which is the probable explanation for its inadequate frequency estimates.

The progressive damage in concrete leading to the frequency reduction can be visualised by contour plots of the post-cracking tensile strains (SCM) or of the damage tension parameter (DPM). Fig. 12 illustrates these damage detection concepts from the analysis example of RC Beam 1. The contours plots outline the zones in concrete affected by cracking and damage

development between the 2.60 kN and 3.72 kN load steps when the steepest 1st mode frequency reduction gradient was measured. Of the two available concrete models and irrespective of the mesh density, the SCM tensile strain plot is more consistent with the observed crack heights of ~ 70 mm (see Fig. 13).

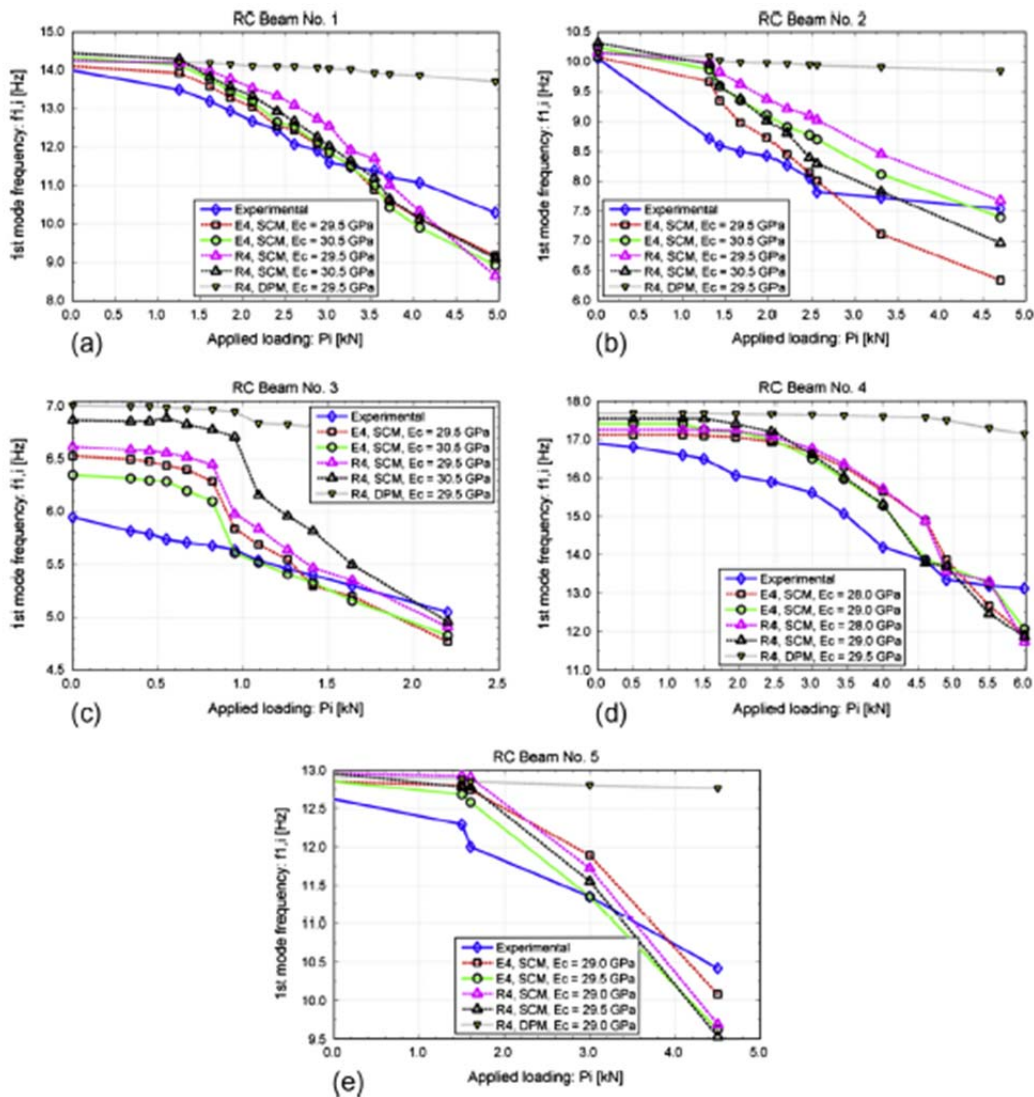


Figure 9: (a)–(e): Load-induced frequency reduction for RC Beams 1 to 5; experimentally measured and 2D FEA computed values.

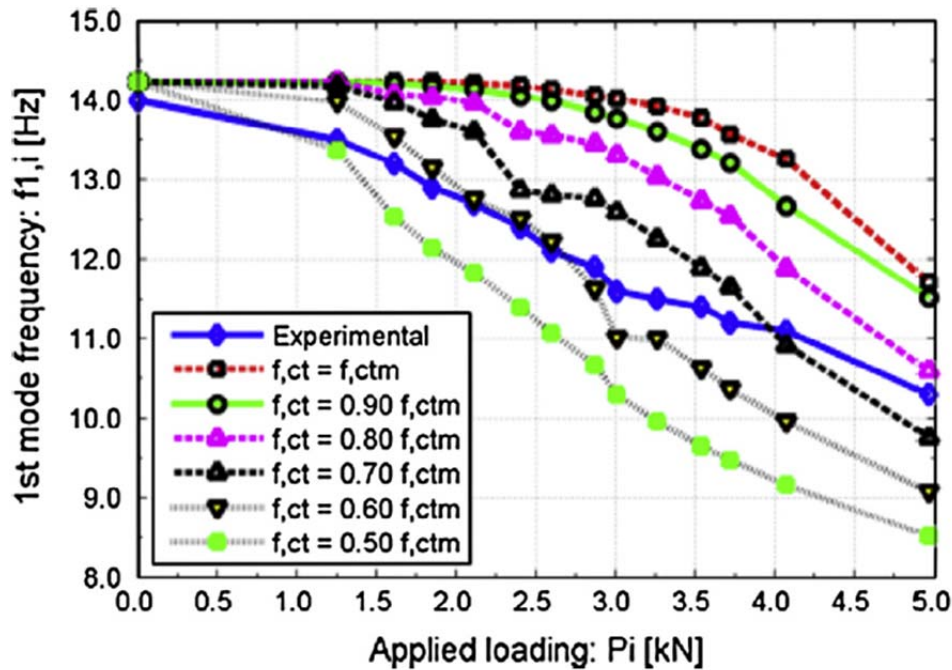


Figure 10: Load-induced 1st mode frequency reduction for RC Beam 1; experimentally measured and 2D FEA computed values with the varying tensile strength of concrete, f_{ct} (SCM with the constant elastic modulus value $E_c=29.5$ GPa).

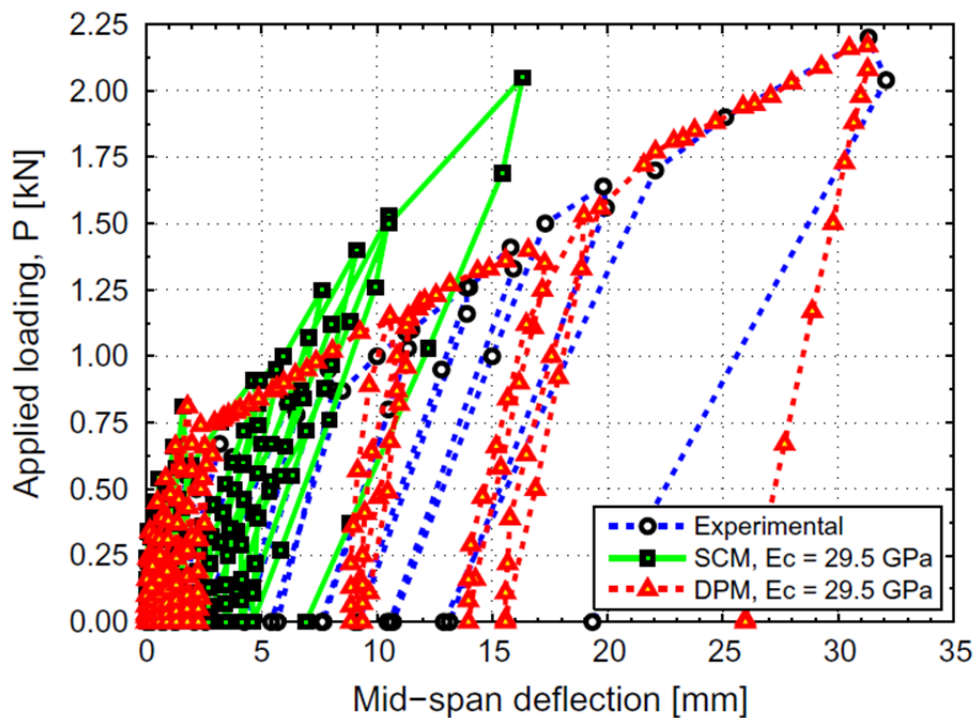


Figure 11: Measured and FEA computed deflection of RC Beam 3 under incremental cycling loading.

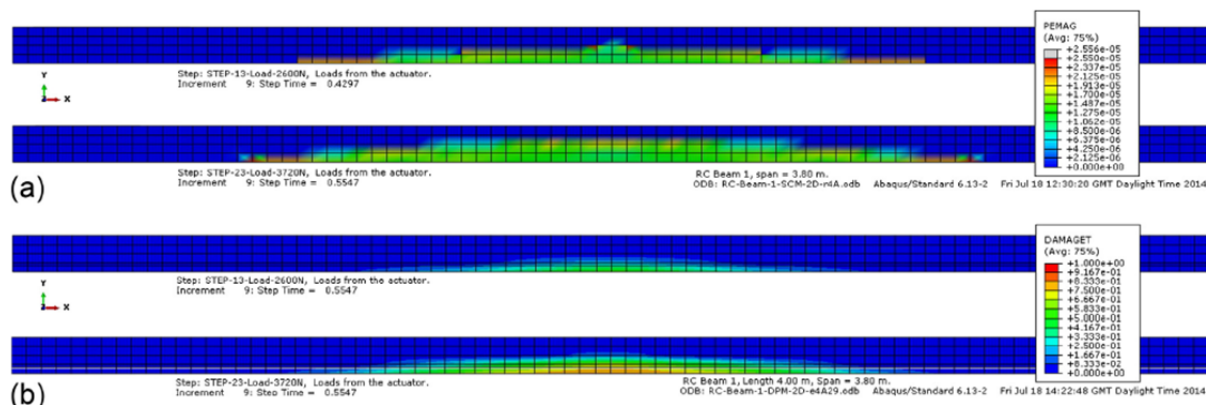


Figure 12: Progression of tensile damage in concrete on RC Beam 1 between 2.60 kN and 3.72 kN load steps ($i=6$ and $i=11$, Table 3); (a) inelastic strains (SCM) and (b) damage variable (DPM).

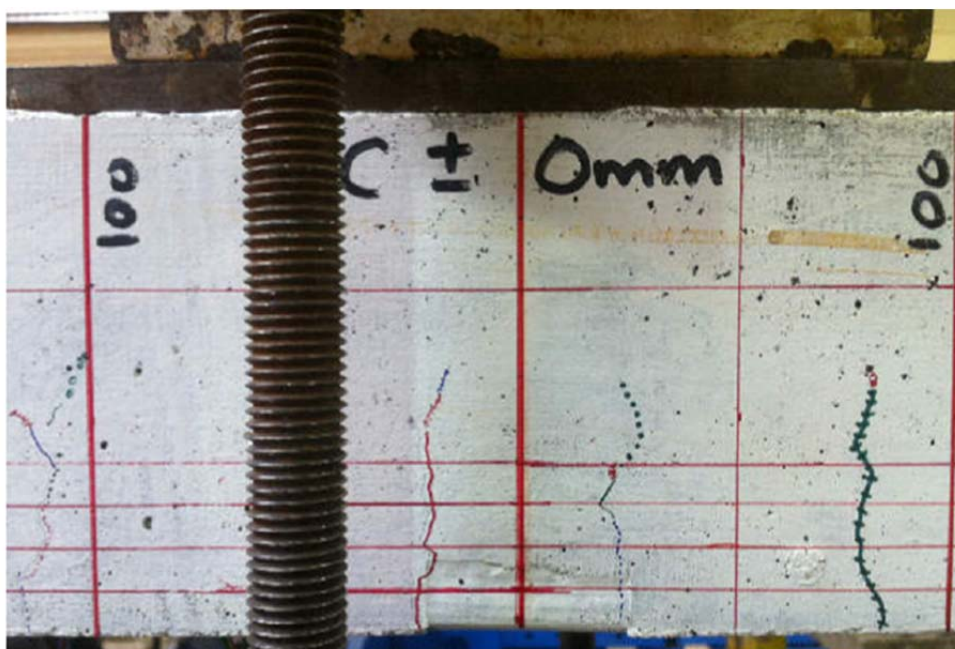


Figure 13: Crack heights at the mid-span of RC Beam 1 (3.72 kN load).

3.2 FE analysis of the two-span RC slab

The concept of applying non-linear FE analysis for the frequency prediction and damage identification is now tried on the independently tested two-span RC slab [12] using two models: 3D solid and shell (Fig. 14), both with embedded steel rebars. The reported compressive strength of concrete is $f_{ck}=33.0$ MPa and the total length, width and thickness of the slab are 6400, 800 and 100 mm, respectively. The longitudinal reinforcement consists of two layers (main tensile and top above the central support); each with $13\varnothing 19$ mm steel bars with the nominal yield strength of 460 MPa.

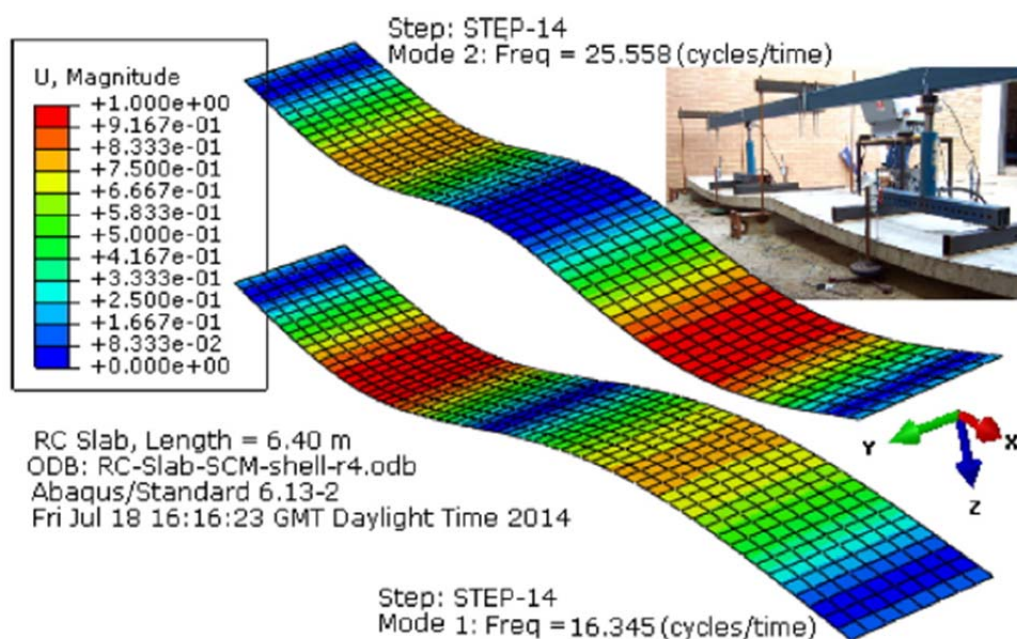


Figure 14: Dynamically tested two-span RC slab [12]; 1st and 2nd natural frequencies after load step 6, from the 3D shell model (Measured vs FEA: 1st mode 16.72 vs. 16.23 Hz; 2nd mode 23.90 vs. 25.56 Hz).

The RC slab was subjected to thirteen non-symmetric load-unload cycles and the maximum loading was 36.0 kN in each of the two 3.2 m spans. The natural frequencies of the 1st and 2nd mode reduced from 17.8 Hz and 25.5 Hz (before the loading) to near 12.0 Hz and 14.0 Hz after the last load-unload step. With the elastic modulus, tensile strength of concrete and the ultimate crack opening displacement values varied as $E_c \approx 27.0\text{--}29.0$ GPa, $f_{ctm} \approx 0.05\text{--}0.06f_{ck}$ and $u_t^{ck} \approx 0.05\text{--}0.08$ mm, the fundamental natural frequencies obtained from the analysis were again found to be in agreement with the experimental measurements within 5% to 10% accuracy as shown in the load–frequency plot in Fig. 15. After the fracture of concrete above the mid-support during the final loading stages, the measured frequency of the 2nd mode converged to that of the 1st mode and this was not accurately predicted by FE analysis. Effectively, the first two vibration modes of the damaged slab reflected the fact that, once the plastic hinge formed above the support, two spans were vibrating almost separately. However, to achieve full analysis convergence, concrete in the FE model was apparently defined with somewhat stiffer fracture properties. As a result, the analytically predicted frequencies at the ultimate loading stages were higher than the experimentally measured. Still, for the earlier load steps, the shell and 3D solid FE models produced frequencies that were in good agreement with the measured

values for the 1st and 2nd vibration mode. Finally, the 3D solid FE model has realistically identified progressive damage in the RC slab that caused frequency reduction (Fig. 16).

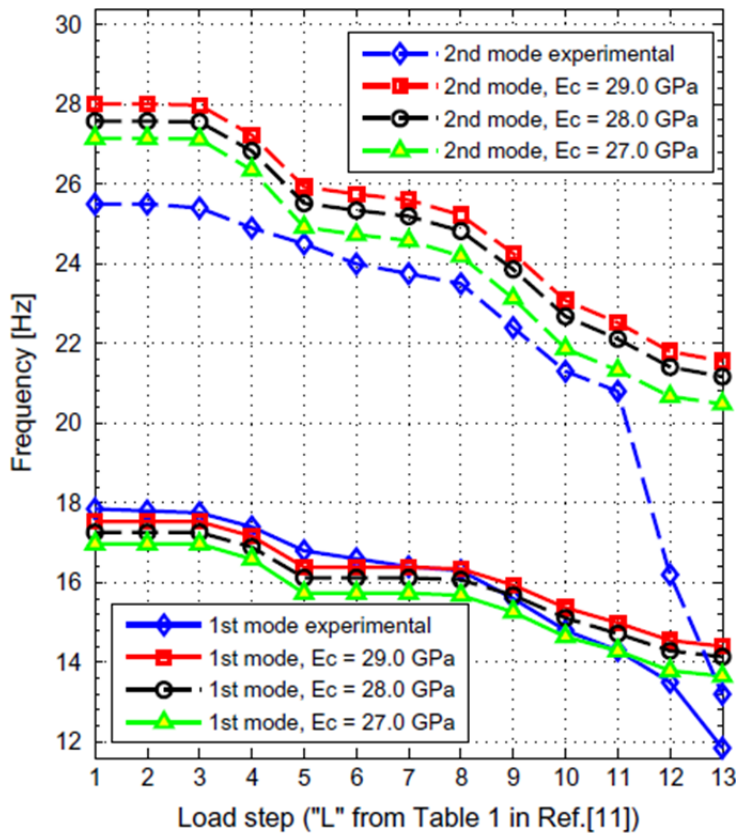


Figure 15: 1st and 2nd mode frequency reduction on incrementally loaded RC slab (experimental and numerical values from the 3D solid FE model).

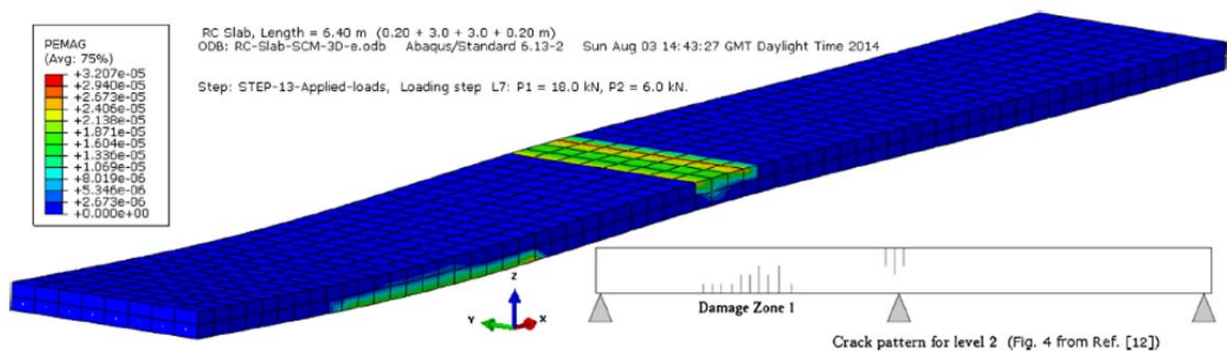


Figure 16: Tensile damage in the two span RC slab (after load step 7).

4 Discussion

The dynamic properties of RC beams (and a slab) were investigated through the study of three inter-linked topics: determination of the modulus of elasticity of concrete, E_c , to be adopted for FE analysis, the rate of frequency reduction under the applied loading and prediction of frequency changes by means of the non-linear FE analysis.

Whilst the static modulus of elasticity of concrete was determined from the cylinder compression tests, there are two more options: to estimate E_c using empirical formulas like Eq. (5) [21] or to derive it indirectly from the dynamic modulus (e.g. the UPV readings on the actual RC structure). For the second case, measurements taken on prisms of different lengths are evidence that, for concrete ages beyond 60 days, the UPV and the dynamic modulus of elasticity, $E_{c,dyn}$ (Eq. (4)), can be considered as material constants. The UPV readings offer a prospect for consistently reliable prediction of the static modulus provided that the r_e ratio (Eq. (6)) is known for a particular concrete mixture but, unfortunately, this is usually not the case.

The modal testing of RC beams was used to correlate the applied incremental loading (and the induced damage) to the reduction of natural frequencies. The slenderness of RC beams, expressed as the span to depth ratio (L_s/h), varied but the change of the measured frequencies presented in the form of the frequency-load graphs (Fig. 5) showed the frequency reduction pattern that is similar to those from the previously published works. The rate of this reduction is faster at the earlier load stages with the maximum drop in measured frequencies, from the initially non-loaded RC beams to the yielding load levels, remaining below 25% for the 1st mode. It is of practical interest to note that, in relative terms, the frequency reduction was relatively larger for the 1st than for the 2nd vibration mode and this was expected given that the beam deflection more resembled the shape of the 1st mode. Furthermore, different static or dynamic load-histories can lead to the same frequency reduction and they need to be known when non-linear FE analysis is used for structural assessment. The argument comes from the application of 100 constant load cycles (at 50% yield level) on RC beam 5 that produced the same cumulative effect on the 1st natural frequency as a single ~20% higher load increment would have.

In the parametric FE analysis performed using ABAQUS, the key variables defined the constitutive laws for concrete in tension. The DPM gives more accurate load–deflections results but is inferior to SCM for the extraction of the reduced beam frequencies. Calculation of the

natural frequencies of RC beams was most sensitive to the values of the initial elastic modulus of concrete, E_c , and the tensile strength of concrete, f_{ct} . Near the median range of tried values (Table 4), variations in the ultimate tensile strain, ϵ_{ctu} , a full crack opening width, u_t^{ck} , and the energy release rate of the 1st fracture mode, G_{fi} , have lesser influence on the calculated post-cracking frequencies. (Example analysis input file for RC beam 2 is provided in Appendix B.) The best frequency predictions using the SCM in the FE analysis were achieved with the initial value of the elastic modulus of concrete adopted $E_c \approx 29.5$ GPa (close to the experimentally obtained static value) and with the tensile strength of concrete near the lower bound defined by Eurocode 2, $f_{ct} \approx 0.70 f_{ctm}$ (Eq. (8)).

Combined with the experimental vibration measurements, the FE analysis of dynamically validated structure models has potential to aid and improve traditionally performed visual inspection and damage assessment of larger RC structures. The proposed vibration based damage assessment framework for the in-service RC structures comprises field modal testing and non-linear FE analysis with the necessary steps summarised in Fig. 17.

When the frequencies are first measured on a newly built structure with known boundary conditions, the value of the elastic modulus of concrete should be verified with the starting FE analysis. Once in exploitation, regular monitoring and periodic modal testing will provide records of the environmental/load history and reduced fundamental frequencies of the incrementally damaged structure. This would allow for the FE model to be updated with the fracture properties of concrete so that the non-linear analysis can match the measured frequencies.

From the analysed examples it follows that, if the values of parameters that define concrete fracture are within the 'narrow' bands that could be identified after the initial damage load levels, the progressive reduction of fundamental frequencies can be reasonably accurately predicted for the later loading stages. The same FE model would then be used for frequency calculation and identification of the damaged zones in concrete which remains the primary

- In dynamic analysis of RC structures, the value of the elastic modulus of concrete, E_c , should be adopted as the modulus obtained from the standard cylinder compression tests.
- For concrete older than 60 days, the ultra-sonic pulse velocity, v_p , and the dynamic modulus of elasticity, $E_{c,dyn}$, can be considered as the material property constants. They could be used for empirical estimation of the concrete compressive strength and static modulus.
- On simply supported RC structures subjected to pure bending (like bridge girders, floor slabs or beams), the damage-induced frequency reduction will be more significant for the 1st mode of vibration.
- Non-linear FE analysis of RC structures modelled with 2D/3D or shell elements can predict the load-induced reduction of their frequencies with the accuracy of $\pm 10\%$. This is consistently achieved with the elastic modulus of concrete adopted as the “static” value E_c and the tensile strength as 5% of the characteristic compressive strength, $f_{ct} \approx 0.05 f_{ck}$.
- The analysis of the RC beams and a slab was performed on the FE models updated with results from the modal testing. The same FE models accurately predicted their future dynamic performance as the damage in concrete was straightforwardly visualised using parameters that define constitutive models in tensions.
- The combined modal and FE analysis methodology can be of particular use in the maintenance of large RC structures on which the full-scale visual inspection is difficult (girders and decks of RC bridges, towers) or when the structural serviceability, rather than integrity, is affected by cracks (liquid retaining RC structures).

Acknowledgements

The authors express gratitude to the University of Warwick for funding the project through its internal Research Development Fund. The thanks are extended to the final year engineering students (class of 2014) and to Dr Peter Little of Admor Engineering (UK) for their help with practical work.

Appendix A. Numerical damage representation for RC Beam 1

A damage scenario for RC Beam 1 after the load steps $i=3,6,11,13$ (Table 3) is plotted in Fig. A.18. It is numerical solution to the beam equation of motion (Eq. (1)) in which the reduction of the cross-sectional second moment of area, from I_0 , and the length of the cracked zone, βL_s , are approximated by the power function [10]: $I(x)=I_0[1-(1-\alpha)\cos^2(t)]$ with $t=(\pi/2)(2x/\beta L_s)^n$. From the linear frame analysis, the “best-fit” frequency results were obtained with the concrete elastic modulus value $E_c=30.5$ GPa. The function $I(x)$ is not unique for a given frequency and ranges for the damage parameter values were $0.80 \leq n \leq 1.50$, $0.70 \geq \alpha \geq 0.45$ and $0.30 \leq \beta \leq 0.65$.

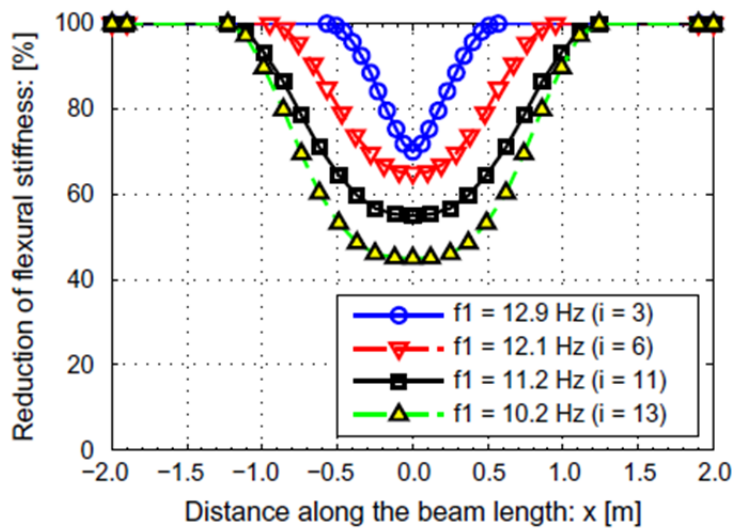


Figure A.18: Representation of the possible damage length and section stiffness reduction for RC Beam 1.

Appendix B. ABAQUS analysis input listing for RC Beam 2

```
*HEADING
RC Beam 2, 2D SCM model with CPS4 + T2D2 elements
*NODE, NSET = EDGE1
  1, -4700., -60.
  2, -4700., -30.
  3, -4700., 0.
  4, -4700., 30.
  5, -4700., 60.
*NODE, NSET = EDGE2
  471, 0., -60.
  472, 0., -30.
  473, 0., 0.
  474, 0., 30.
  475, 0., 60.
*NFILL, NSET = Concrete_nodes_4
EDGE1, EDGE2, 94, 5
*NODE
  476, -4700., -40.
  570, 0., -40.
*NGEN, NSET = REBAR_NODES
  476, 570, 1
*NSET, NSET = Fixed_support_node
  11
*NSET, NSET = Roller_support_node
  461
*NSET, NSET = Mid_span_node
  236
*ELEMENT, TYPE = CPS4
  1, 1, 6, 7, 2
*ELGEN, ELSET = Set-Con
  1, 4, 1, 1, 94, 5, 4
*ELEMENT, TYPE = T2D2
  377, 476, 477
*ELGEN, ELSET = REBAR_1
  377, 94, 1, 1
*ELSET, ELSET = Set-CONEL, GENERATE
  1, 373, 4
*ELSET, ELSET = EL-loaded
  184, 188, 192, 196
*SURFACE, TYPE = ELEMENT, NAME = Surf-Pressure
  EL-loaded, S3
*EMBEDDED ELEMENT, HOST ELSET = Set-CONEL
  REBAR_1
*SOLID SECTION, ELSET = Set-Con, MATERIAL = Concrete
  300.,
*SOLID SECTION, ELSET = REBAR_1, MATERIAL = Steel
  235.62
*MATERIAL, NAME = Steel
*DENSITY
  7.85e-09,
*ELASTIC
  200000., 0.3
```

```

*PLASTIC
553., 0.
560., 0.002095
600., 0.003880
625., 0.011000
*MATERIAL, NAME = Concrete
*DENSITY
2.31e-09,
*ELASTIC
29500., 0.2
*CONCRETE
21.20, 0.
32.49, 0.000049
40.38, 0.000187
46.16, 0.000379
50.07, 0.000619
52.29, 0.000903
53.00, 0.001227
52.70, 0.001463
51.83, 0.001714
49.52, 0.002117
30.00, 0.003500
*FAILURE RATIOS
1.15, 0.045, 1.25, 0.33
*TENSION STIFFENING, TYPE = DISPLACEMENT
0.05
*SHEAR RETENTION
1.00, 0.01
*BOUNDARY
Fixed_support_node, 1, 1
Fixed_support_node, 2, 2
Roller_support_node, 2, 2
*AMPLITUDE, NAME = LOAD_UNLOAD,
    DEFINITION = TABULAR
    0.0, 0.0, 0.125, 0.25, 0.25, 0.5, 0.375, 0.75
    0.5, 1.0, 0.625, 0.75, 0.75, 0.5, 0.875, 0.25
    1.0, 0.0
** -----
*STEP, NAME = STEP-1-Self-weight, NLGEOM = YES,
    INC = 2
    Self-weight (gravity) loading only, i = 0.
*STATIC, DIRECT
0.5, 1.,
*DLOAD
    , GRAV, 9810., 0., -1., 0.
*OUTPUT, FIELD, VARIABLE = ALL
*OUTPUT, HISTORY, FREQUENCY = 1
*END STEP
** -----
*STEP, NAME = STEP-2-Freq, NLGEOM = YES,
    PERTURBATION
    Frequencies of the non-loaded beam
*FREQUENCY, NORMALIZATION = DISPLACEMENT
10., , ,
*RESTART, WRITE, FREQUENCY = 0
*OUTPUT, FIELD, VARIABLE = PRESELECT
*END STEP
** -----

```



```
*STEP, NAME = STEP-3-Load-1310 N, NLGEOM = YES,
  INC = 500
  Loads from the actuator,  $i = 1 \rightarrow P_i = 1310 \text{ N}$ .
*STATIC, STABILIZE
  0.025, 1., 0.00001, 0.15
** Pressure area mid-span, 4 el. x 50 mm x 300 mm
** Surf-pressure  $P = P_i / (4 * 50 * 300) \text{ N/mm}^2$ 
*DSLOAD, AMPLITUDE = LOAD_UNLOAD
  Surf-Pressure, P, 0.0218
*MONITOR, DOF = 2, NODE = Mid_span_node, FREQUENCY = 1
*OUTPUT, FIELD, VARIABLE = ALL
*OUTPUT, HISTORY, FREQUENCY = 1
*END STEP
** -----
*STEP, NAME = STEP-4-Freq, NLGEOM = YES,
  PERTURBATION
  Freq. of the CRACKED BEAM AFTER 1310 N LOADING
*FREQUENCY, NORMALIZATION = DISPLACEMENT
  10,, , ,
*RESTART, WRITE, FREQUENCY = 0
*OUTPUT, FIELD, VARIABLE = PRESELECT
*END STEP
** -----
** Repeat command blocks of STEPS 3 and 4
** for the remaining loading stages  $i := 2$  to 8.
** (See Table 3,  $P_i$  entries for RC Beam 2.)
** -----
```

References

- [1] Jerath S, Sibani MM. Dynamic modulus for reinforced concrete beams. *J Struct Eng* 1984;110(6):1405–10.
- [2] Casas JR. An experimental study on the use of dynamic tests for surveillance of concrete structures. *Mater Struct* 1994;27(10):588–95.
- [3] Shkolnik IE. Effect of nonlinear response of concrete on its elastic modulus and strength. *Cement Concrete Compos* 2005;27(7–8):747–57.
- [4] Qixian L, Bungey JH. Using compressive wave ultrasonic transducers to measure the velocity of surface waves and hence determine dynamic modulus of elasticity for concrete. *Constr Build Mater* 1996;10(4):237–42.
- [5] Popovics JS, Zemajtis J, Shkolnik I. A study of static and dynamic modulus of concrete. ACI-CRC Final Report, American Concrete Institute; October 2008.
- [6] Han S-H, Kim J-K. Effect of temperature and age on the relationship between dynamic and static elastic modulus of concrete. *Concrete Cement Res* 2004;34(7):1219–27.
- [7] Lu X, Sun Q, Feng W, Tian J. Evaluation of dynamic modulus of elasticity of concrete using impact-echo method. *Constr Build Mater* 2013;47:231–9.
- [8] Musiał M. Static and dynamic stiffness of reinforced concrete beams. *Arch Civil Mech Eng* 2012;12(2):186–91.
- [9] Euronorm 1992-1-1: 2004, Eurocode 2 – design of concrete structures. Part 1-1: General rules and rules for buildings, Comité Européen de Normalisation (CEN), Brussels; 2004.
- [10] Maeck J, Wahab MA, Peeters B, De Roeck G, De Visscher J, De Wilde WP, Ndambi J-M, Vantomme J. Damage identification in reinforced concrete structures by dynamic stiffness determination. *Eng Struct* 2000;22(10): 1339–49.

- [11] Neild SA, Williams MS, McFadden PD. Nonlinear vibration characteristics of damaged concrete beams. *J Struct Eng* 2003;129(2):, 260–268.
- [12] Zhu X, Hao H. Damage detection of RC slabs using nonlinear vibration features. *Int J Struct Stab Dynam* 2009;9(4):687–709.
- [13] Massenzio M, Jacquelin E, Ovigne PA. Natural frequency evaluation of a cracked RC beam with or without composite strengthening for a damage assessment. *Mater Struct* 2005;38(10):, 865–873.
- [14] Wang Z, Man XC, Finch RD, Jansen BH. The dynamic behavior and vibration monitoring of reinforced concrete beams. *J Testing Eval* 1998; 26(5):405–19.
- [15] Koh SJA, Maleej M, Quek ST. Damage quantification of flexurally loaded RC slab using frequency response data. *Struct Health Monit* 2004;3(4):293–311.
- [16] Salawu OS. Detection of structural damage through changes in frequency: a review. *Eng Struct* 1997;19(9):718–23.
- [17] Carden EP, Fanning P. Vibration based condition monitoring: a review. *Struct Health Monit* 2004;3(4):355–77.
- [18] Pavic A, Reynolds P, Waldron P, Bennett K. Dynamic modelling of posttensioned concrete floors using finite element analysis. *Fin Elem Anal Des* 2001;37(4):305–23.
- [19] Consuegra F, Irfanoglu A. Variation of small amplitude vibration dynamic properties with displacement in reinforced concrete structures. *Exp Mech* 2012;52(7):817–28.
- [20] Sousa C, Calçada R, Neves AS. Numerical evaluation of the non-linear behaviour of cracked RC members under variable-amplitude cyclic loading. *Mater Struct*; 11 June 2014.
- [21] Noguchi T, Tomosawa F, Nemati KM, Chiaia BM, Fantilli AP. A practical equation for elastic modulus of concrete. *ACI Struct J* 2009;105(5):690–6.
- [22] ABAQUS v6.13-2. Analysis users manual, Dassault Systèmes, Providence, RI, USA; 2013.
- [23] Lee J, Fenves GL. Plastic-damage model for cyclic loading of concrete structures. *J Eng Mech* 1998;124(8):892–900.